ap

Asian Journal of Physics
Vol. 29, Nos 3&4 (2020) 249-254
Available on: www.asianjournalofphysics.in

Integrated digital holographic and atomic force microscope for refractive index characterization of microscopic objects

N Cardenas and S K Mohanty
Nanoscope Technologies LLC, 1312 Brown Trail Bedford, TX 76022.

This article is dedicated to Prof Pradeep K Gupta for his contributions to optics and photonics with biomedical applications

Refractive index characterization of both living and non-living microscopic objects is of significant interest for variety of biomedical applications. Here, we report use of an integrated Atomic force microscope (AFM) and Digital holographic microscope (DHM) for refractive index mapping. Though DHM yields quantitative phase properties of the sample with high temporal resolution, the phase measurements are inherently dependent on both the refractive index and physical thickness. Integration of DHM and AFM on the same inverted microscope led to realization of a powerful platform for nanoscale mapping of phase and thickness of microscopic samples.

Keywords: Digital holographic microscopy, Atomic Force Microscope, Refractive index mapping, Surface topography, Nanoscopic imaging.

1 Introduction

Refractive index characterization of both living and non-living microscopic objects is of significant interest for variety of material science and biomedical applications. For example, microspheres of high [1] as well as low [2-3] refractive indices have been finding importance as contrast enhancement agents for optical coherence tomography as well as other (e.g. ultrasound) modes of imaging. Further, significant changes in refractive index of living cells (especially, red blood cells) are known to occur under influence of number of diseases such as malaria [4], cancer [5], and diabetes [6]. Therefore, measurement of the change in refractive index of cells can lead to better understanding of disease progression as well as pathological characterization [7]. Though digital holographic microscopy [8-9] (DHM), allows wide-field recording of the quantitative phase of the samples with high axial resolution, the refractive index and physical thickness values are not decoupled. Therefore, quantitative phase imaging methods [10] generally assumes either thickness or refractive index of the sample in order to determine the other parameter from the phase. Recently, we reported a dual-medium method [11] for decoupling refractive index from physical thickness. However, it requires change of medium surrounding the microscopic object and therefore may not be acceptable in many situations. For the purpose of determining thickness and refractive index of microscopic objects without changing the medium, we integrated atomic force microscopy (AFM) imaging [12] with DHM on same microscope platform. While such measurements have been carried out earlier on independent platforms, the integrated system has distinct advantages of *in-situ* characterization and manipulation of microscopic samples. The integrated AFM-DHM system was employed to characterize polystyrene microspheres and red blood cells.

Digital holography, an emergent wide-field imaging technique, offers high axial resolution for quantitative phase imaging. In this method, a hologram that consists of the interference between the object and the reference beams is recorded by a CCD camera and the holographic image is numerically

Corresponding author :
*e mail:*smohanty@nanoscopetech.com (S K Mohanty)

reconstructed using the results of diffraction theory. Calculation of the complex optical field allows direct access of both the amplitude and phase information of the optical field, and by numerical focusing; the images can be obtained at any distance from a single recorded hologram. Digital holography also affords numerous digital processing techniques for manipulating the optical field information such as curvature in ways that are difficult or impossible in real space processing. For numerical reconstruction in digital holographic imaging, the propagation of the optical field can be calculated based on the Fresnel diffraction formula. The holographic image is numerically reconstructed using the angular spectrum method. Briefly, the angular spectrum of the wave field is obtained by taking the Fourier transform of electric field and separating it from other spectral components of the hologram with a band-pass filter by adjusting the off-axis angle θ of the incident beam. Then, the modified field can be rewritten as the inverse Fourier transform of the filtered angular spectrum. Thus the complex field distribution $E(x,y,z)$ of any plane perpendicular to the propagating z axis can be calculated from Fourier theory [13]. The resolution of the reconstructed images from the angular spectrum method is the same as that in the hologram plane. The non-ambiguity phase range calculated from the complex field distribution is only from $-\pi$ to π. Any phase outside this range will cause a wrapping effect of the phase map. The 2π phase ambiguities can be directly resolved to get an absolute sample phase map by phase unwrapping using Goldstein's algorithm [14]. From the quantitative phase information, the refractive index (n) of the microscopic object was estimated from the physical thickness (Δd) using the equation $\Delta d = \lambda(\Delta\varphi/2\pi)/(n - n_0)$, where λ is the wavelength, $\Delta\varphi$ is the phase, and n_0 is the refractive index of the surrounding medium.

2 Result and Discussion

To enable simultaneous height and phase imaging of the sample, the integrated AFM-DHM system was built on the same inverted microscope. The schematic of the system is shown in Fig 1. The optically transparent fiber optic cantilever-tip of the AFM (Multiview, Nanonics) allowed successful integration of the DHM with the AFM. The mirror (M1) reflects the diode laser (DL) beam on to the fiber-tip. The reflection from the tip is detected by a quadrant photodiode (QPD) interfaced with PC. For holographic imaging, a diode laser (Micro Laser Systems) with an output wavelength of 670nm was used. The beam was collimated and expanded with a beam expander and split by a beam splitter (BS1) for Mach-Zehnder interferometry. One beam is directed to illuminate the sample through a condenser (CL) as would be done for transmission mode microscopy. The beam splitter transmits white light from halogen lamp (HAL) for bright-field imaging. The transmitted light is imaged by CCD1. The reference beam transmitted through BS1 is routed via a lens (L) and mirror (M2) to impinge on another beam splitter (BS2). The transmitted sample beam is deflected to the right by use of a mirror (M3) for allowing interference with the reference beam, which is recorded in the right-CCD2. Another microscope objective was placed in the reference arm of the interferometer for curvature compensation (not shown in picture). A slight angle is introduced between the object and the reference beams for off-axis holography. The holographic diffraction pattern and phase images were calculated in real time using custom-made software based on LabVIEW®. The AFM images were processed using *WSxM*software [15].

Polystyrene microspheres, and discotic RBCs (in an isotonic solution) were used for the AFM-DHM based refractive index characterization experiments. The samples were placed on the AFM piezo stage (Multiview, Nanonics), which was then mounted on the microscope sample platform. The piezo stage was controlled by the computer. Figure 2 shows DHM and AFM imaging of polysterene particles (Bangs Lab). The AFM intensity (height) map of one of the polystyrene particles (Fig 2a) is shown in Fig 2b. The 3D topographic reconstruction is carried out using *WSxM* software [15]. In order to determine the phase of the particles, simultaneous DHM imaging of the particles was carried out. The wrapped phase map obtained using DHM and corresponding unwrapped quantitative phase map in 3D are shown in Figs (2c) and (2d), resepectively. Figure (2e) shows the quantitative phase profile (green line) along a line across one of the

particles. The height profile of the same particle along the line (drawn in Fig 2b) is also shown in Fig (2e) (black line). The optical thickness obtained from DHM-phase value is divided by physical thickness (AFM) to obtain refractive index map. The calculated refractive index profile of the polystyrene particle along the line is shown in Fig 2e (red line).

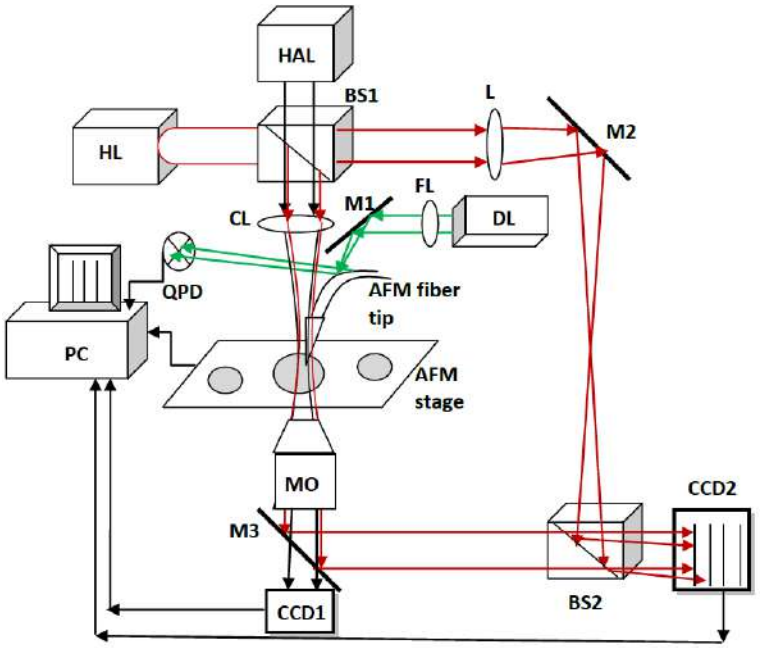

Fig 1. Schematic of the integrated AFM and DHM set up on an inverted microscope platform. HL: Holographic laser for DHM; BS1 and BS2: Beam splitters; L: Lens; HAL: Halogen Lamp; CL: Condenser lens; DL: Diode laser; FL: Focussing lens; QPD: Quadrant photo diode; MO: Microscope objective; M1-3: Mirrors.

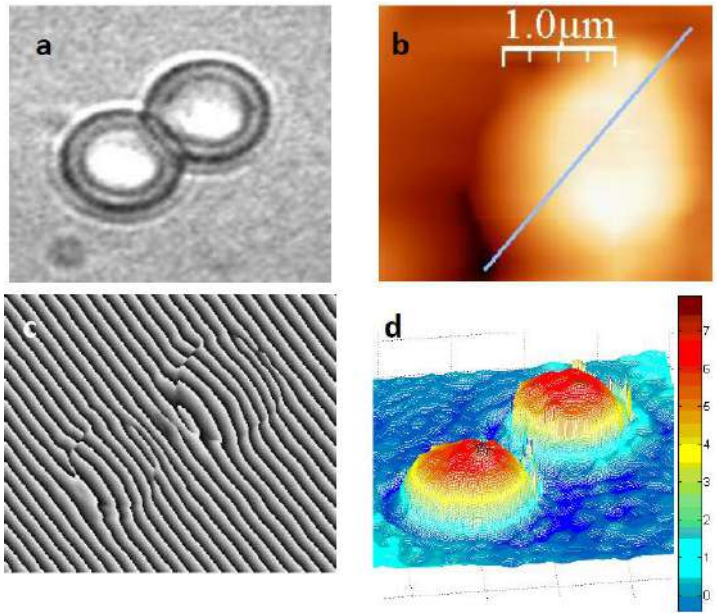

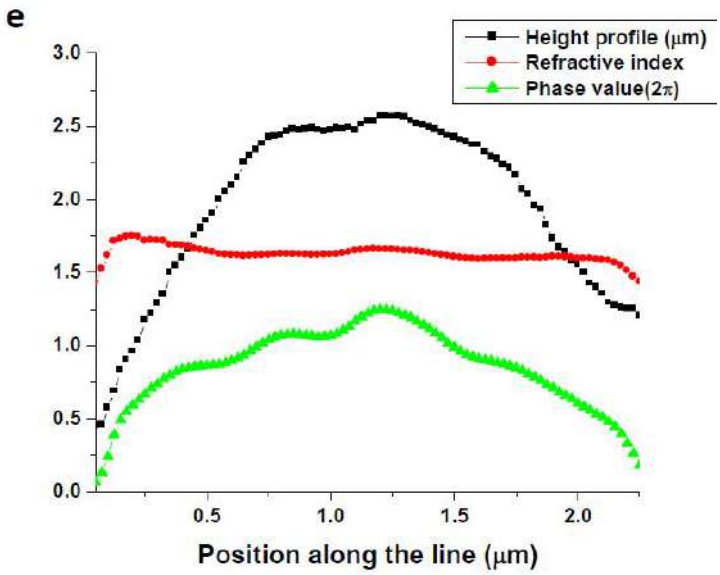

Fig 2. Height and refractive index characterization of of polysterene microsphere using AFM-DHM. (a) Bright field image, (b) AFM intensity (height) map. (c) Wrapped phase map from DHM, and (d) unwrapped quantitative phase map in 3D. (e) Phase (green line), height (black line) and refractive index (red line) profile of a polystyrene particle along a line.

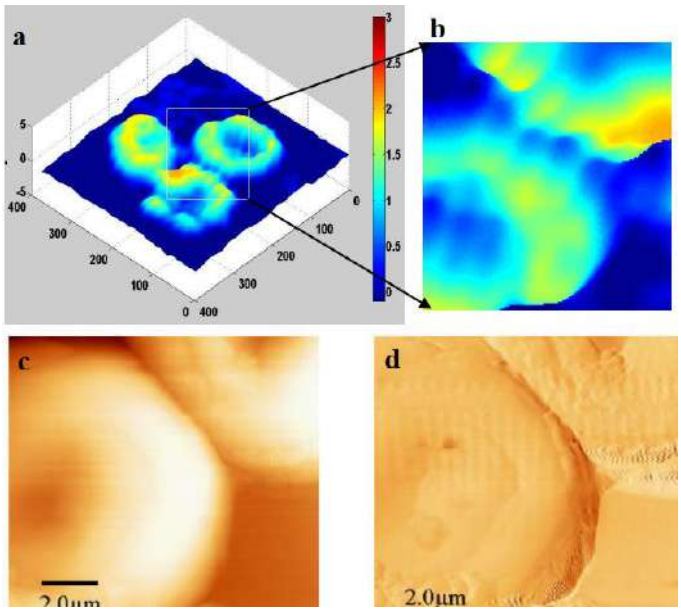

Fig 3. DHM-AFM imaging of red blood cells (RBCs). (a) Quantitative phase map (DHM) of three RBCs, (b) Zoomed phase image of a region of interest. (c) AFM Intensity (height) map of the region of interest, (d) AFM phase image of the RBCs.

Figure 3 shows integrated DHM-AFM imaging of red blood cells. The quantitative phase map (DHM) of three RBCs are shown in Fig (3a). Figure (3b) shows the zoomed phase image of a region of

interest. In Fig (3c), we show intensity (height) map of the region of interest obtained by AFM. Figure (3d) shows AFM phase image of the RBCs. While AFM provides nm-resolution mapping of physical thickness, it requires significant recording time for examination of wide sample area owing to the scanning nature of the recording method. However, accurate determination of the refractive index map from the DHM required estimation of the physical thickness of the sample by AFM. Once refractive index is quantified, DHM can be used for measurement of dynamic changes in physical thickness over a wide-area with high temporal resolution. Unlike AFM, transverse resolution of DHM is limited by the optical diffraction limit. Therefore, integration of DHM with AFM can provide nanoscale information (refractive index, physical thickness).

While mapping of refractive index (a fundamental property for material characterization) will allow wide-area evaluation of changes in parameters such as temperature, density (e.g. biomolecular interactions), measurement of dynamic physical changes will allow estimation of surface uniformity, viscoelastic properties of cells, and will also allow imaging of other dynamic events during mechanical actuation by the AFM cantilever. Since the pathophysiology of progression of diseases such as cancer is reflected in the material properties of the cells, it will be possible to quantify such changes optically by measurement of refractive index and viscoeleastic properties.

3 Conclusion

To conclude, DHM in combination with AFM allowed comprehensive evaluation of height and refractive index of microscopic objects. The transparent nature of the fiber-optic AFM cantilever allowed simultaneous bright field/phase contrast imaging of the sample. The setup was utilized for refractive index and topographic analysis of microscopic objects.

References

1. Lee T M, Oldenburg A L, Sitafalwalla S, Marks D L, Luo W, Toublan F J J, Suslick K S, Boppart S A, Engineered microsphere contrast agents for optical coherence tomography, *Opt Lett*, 28(2003)1546-1548.
2. Klibanov A L, Targeted delivery of gas-filled microspheres, contrast agents for ultrasound imaging, *Adv Drug Deliver Rev*, 37(1999)139-157.
3. Barton J K, Hoying J B, Sullivan C J, Use of microbubbles as an optical coherence tomography contrast agent, *Acad Radiol*, 9(2002)S52-S55.
4. Park Y, Diez-Silva M, Popescu G, Lykotrafitis G, Choi W, Feld M S, Suresh S, Refractive index maps and membrane dynamics of human red blood cells parasitized by Plasmodium falciparum, *PNAS*, 105(2008)13730-13735.
5. Hoyt K, Castaneda B, Zhang M, Nigwekar P, di Sant'agnese P A, Joseph J V, Strang J, Rubens D J, Parker K J, Tissue elasticity properties as biomarkers for prostate cancer, *Cancer Biomark*, 4(2008)213-225.
6. Airaksinen K E J, Salmela P I, Linnaluoto M K, Ikäheimo M J, Ahola K, Ryhänen L J, Diminished arterial elasticity in diabetes: association with fluorescent advanced glycosylation end products in collagen, *Cardiovascular Research*, 27(1993)942-945.
7. Kang J W, Lue N, Kong C R, Barman I, Dingari N C, Goldfless S J, Niles J C, Dasari R R, Feld M S, Combined confocal Raman and quantitative phase microscopy system for biomedical diagnosis, *Biomed Opt Express*, 2(2011)2484-2492.
8. Cuche E, Bevilacqua F, Depeursinge C, Digital holography for quantitative phase-contrast imaging, *Opt Lett*, 24(1999)291-293.
9. Yu L F, Mohanty S, Zhang J, Genc S, Kim M K, Berns M W, Chen Z P, Digital holographic microscopy for quantitative cell dynamic evaluation during laser microsurgery, *Opt Express*, 17(2009)12031-12038.
10. Cardenas N, Kumar S, Mohanty S, *Appl Phys Lett*, 101(2012)203702-203704.
11. Cardenas N, Mohanty S, Decoupling of geometric thickness and refractive index in quantitative phase microscopy, *Opt Lett*, 38(2013)1007-1009.
12. Binnig G, Quate C F, Gerber C, Atomic force microscope, *Phys Rev Lett*, 56(1986)930-933.

13. Goodman J W, Introduction to Fourier optics, 2nd edn, (McGraw-Hill, New York), 1996.
14. Goldstein R M, Zebker H A, Werner C L, Satellite radar interferometry: two-dimensional phase unwrapping, *Radiol Sci*, 23(1988)713-720.
15. Horcas I, Fernandez R, Gomez-Rodriguez J M, Colchero J, Gomez-Herrero J, Baro A M, WSXM: A software for scanning probe microscopy and a tool for nanotechnology, *Rev Sci Instrum*, 78(2007)013705; doi. org/10.1063/1.2432410.

[*Received*: 01.03.2020; *accepted*: 10.03.2020]

Samarendra Mohanty

Dr Samarendra Mohanty, is Founder-President and Chief Scientific Officer of Nanoscope Technologies and Nanoscope Therapeutics, CEO of Nanoscope Instruments and Nanoscope Diagnostics and CTO of Opsin Biotherapeutics. He is an Adjunct Professor at North Texas Eye Research Institute at UNT Health Science Center and former Professor (Physics) at University of Texas, who held positions as Senior Scientist at RRCAT, Government of India and in various reputed institutions. Dr. Mohanty is an inventor with many patents and serial entrepreneur and has successfully commercialized several products. He has decades of experience on Biomedical technologies in Asia, Europe and US. He has authored over 200 publications in journals and conferences. His research findings have been highlighted in hundreds of websites and magazines including New Scientists, Nature Photonics, Wall street journal, Biophotonics, and Laser focus world. The innovative research by Dr Mohanty is funded by National Institute of Health, National Science Foundation, currently he is the PI on major grants from US National Eye Institute's Audacious Goal Initiative and Bioengineering Research grants. He serves on the editorial board of reputed journals and chairs international conference on optogenetics. He is spearheading the clinical studies and commercialization of optogenetic therapies and label-free cancer diagnostics. He has received many awards including 2019 Healthcare Heroes award from Fort Worth Business Press.

Nelson Cardenas

Nelson Cardenas obtained B S with Major in Physics and Minor in Mechanical and Aerospace Engineering from University of Texas at Arlington. His research interest includes Optical metrology and characterization of materials. He shared the Robert S Hyer award in 2011 with Dr Samarendra Mohanty given by American Physical Society.